Thin accretion disks in $f(R)$ modified gravity models

C. S. J. Pun[1],* Z. Kovács[2,3],† and T. Harko[1‡]

[1]*Department of Physics and Center for Theoretical and Computational Physics, The University of Hong Kong, Pok Fu Lam Road, Hong Kong*

[2]*Max-Planck-Institute für Radioastronomie, Auf dem Hügel 69, 53121 Bonn, Germany and*

[3]*Department of Experimental Physics, University of Szeged, Dóm Tér 9, Szeged 6720, Hungary*

(Dated: June 13, 2013)

Abstract

We consider the basic physical properties of matter forming a thin accretion disc in the static and spherically symmetric space-time metric of the vacuum $f(R)$ modified gravity models. The Lagrangian of the generalized gravity theory is also obtained in a parametric form, and the conditions of the viability of the model are discussed. The exact Schwarzschild type solution of the gravitational field equations in the $f(R)$ gravity contains a linearly increasing term, as well as a logarithmic correction, as compared to the standard Schwarzschild solution of general relativity, and it depends on four arbitrary integration constants. The energy flux and the emission spectrum from the accretion disk around the $f(R)$ gravity black holes are obtained, and they are compared to the general relativistic case. Particular signatures can appear in the electromagnetic spectrum, thus leading to the possibility of directly testing modified gravity models by using astrophysical observations of the emission spectra from accretion disks.

PACS numbers: 04.50.Kd, 04.70.Bw, 97.10.Gz

*Electronic address: jcspun@hkucc.hku.hk

†Electronic address: zkovacs@mpifr-bonn.mpg.de

‡Electronic address: harko@hkucc.hku.hk

I. INTRODUCTION

Several recent astrophysical observations [1] have provided the astonishing result that around 95–96% of the content of the Universe is in the form of dark matter + dark energy, with only about 4–5% being represented by baryonic matter. More intriguing, around 70% of the energy-density may be in the form of what is called "dark energy", and is responsible for the acceleration of the distant type Ia supernovae [2]. Hence, today's models of astrophysics and cosmology face two severe problems, that can be summarized as the dark energy problem, and the dark matter problem, respectively. Although in recent years many different suggestions have been proposed to overcome these issues, a satisfactory answer has yet to be obtained.

A very promising way to explain these major problems is to assume that at large scales the Einstein gravity model of general relativity breaks down, and a more general action describes the gravitational field. Theoretical models in which the standard Einstein-Hilbert action is replaced by an arbitrary function of the Ricci scalar R, first proposed in [3], have been extensively investigated lately. The only restriction imposed on the function f is to be analytic, that is, it must possess a Taylor series expansion about any point. Cosmic acceleration can be explained by $f(R)$ gravity [4], and the conditions of viable cosmological models have been derived in [5]. In the context of the Solar System regime, severe weak field constraints seem to rule out most of the models proposed so far [6, 7], although viable models do exist [8, 9, 10, 11]. The possibility that the galactic dynamic of massive test particles can be understood without the need for dark matter was also considered in the framework of $f(R)$ gravity models [12, 13, 14, 15, 16], and connections with MOND and the Pioneer anomaly further explored by considering an explicit coupling of an arbitrary function of R with the matter Lagrangian density [17, 18]. For a recent review of the $f(R)$ modified gravity models see [19].

The study of the static spherically symmetric vacuum solutions of the gravitational field theories is fundamental for the physical understanding and interpretation of the model. In particular, the vacuum solutions provide the theoretical basis for the Solar System testing of the theories, and for the description of the motion of the test particles around massive bodies. It was shown that for a large class of models, including e.g. the $f(R) = R - \mu^4/R$ model, the Schwarzschild-de Sitter metric is an exact solution of the field equations. Solutions in

the presence of a perfect fluid were analyzed in [20]. Other approaches in searching for exact spherically symmetric solutions of $f(R)$ theories of gravity were studied in [21], respectively.

Several exact vacuum static and spherically symmetric solutions of the gravitational field equations in $f(R)$ gravity were obtained in [23]. The set of the modified Einstein's field equations were reduced to a single, third order differential equation, and it was shown how one can construct exact solutions in different $f(R)$ models. In particular, a Schwarzschild type solution of the field equation was constructed. This solution, containing a term linearly increasing with the radial coordinate, as well as a logarithmic term, depends on four new arbitrary integration constants, and reduces to the standard general relativistic case by imposing the zero value to one integration constant, and by appropriately choosing the numerical values of the other constants. However, even that this choice of constants allows the model to pass the solar system tests, we expect that at large distances, or in the presence of strong gravitational fields, the geometry of the space-time in $f(R)$ modified gravity models is different from that of standard general relativity. Therefore, it is important to find a method that could allow one to observationally distinguish, and test in an astrophysical setting, the possible deviations from Einstein's theory. One such possibility is the study of accretion disks around compact objects.

Most of the astrophysical bodies grow substantially in mass via accretion. Recent observations suggest that around almost all of the active galactic nuclei (AGN's), or black hole candidates, there exist gas clouds surrounding the central compact object, together with an associated accretion disc, on a variety of scales from a tenth of a parsec to a few hundred parsecs [25]. These gas clouds are assumed to form a geometrically and optically thick torus (or warped disc), which absorbs most of the ultraviolet radiation and the soft X-rays. The gas exists in either the molecular or the atomic phase. The most powerful evidence for the existence of super massive black holes comes from the VLBI imaging of molecular H_2O masers in the active galaxy NGC 4258 [26]. This imaging, produced by Doppler shift measurements assuming Keplerian motion of the masering source, has allowed a quite accurate estimation of the central mass, which has been found to be a $3.6 \times 10^7 M_\odot$ super massive dark object, within 0.13 parsecs. Hence, important astrophysical information can be obtained from the observation of the motion of the gas streams in the gravitational field of compact objects.

The mass accretion around rotating black holes was studied in general relativity for the

first time in [27]. By using an equatorial approximation to the stationary and axisymmetric space-time of rotating black holes, steady-state thin disk models were constructed, extending the theory of non-relativistic accretion [28]. In these models hydrodynamical equilibrium is maintained by efficient cooling mechanisms via radiation transport, and the accreting matter has a Keplerian rotation. The radiation emitted by the disk surface was also studied under the assumption that black body radiation would emerge from the disk in thermodynamical equilibrium. The radiation properties of the thin accretion disks were further analyzed in [29] and in [30], where the effects of the photon capture by the hole on the spin evolution were presented as well. In these works the efficiency with which black holes convert rest mass into outgoing radiation in the accretion process was also computed.

Later on, the emissivity properties of the accretion disks were investigated for exotic central objects, such as non-rotating or rotating quark, boson or fermion stars [31, 32, 33]. The radiation power per unit area, the temperature of the disk and the spectrum of the emitted radiation were given, and compared with the case of a Schwarzschild black hole of an equal mass.

It is the purpose of the present paper to study the thin accretion disk models applied for black holes in $f(R)$ modified gravity models, and carry out an analysis of the properties of the radiation emerging from the surface of the disk.

The present paper is organized as follows. The $f(R)$ gravity generalization of the Schwarzschild type solution of general relativity is obtained in Section II. In Section III we review the formalism of the thin disk accretion onto compact objects. The basic properties of matter forming a thin accretion disc in the space-time metric of the $f(R)$ modified gravity models are considered in Section IV. We discuss and conclude our results in Section V. In the present paper we use a system of units so that $c = G = \hbar = k_B = 1$, where k_B is Boltzmann's constant.

II. VACUUM FIELD EQUATIONS IN $f(R)$ GRAVITY

In the $f(R)$ gravity models the gravitational action is given by

$$S = \int f(R)\sqrt{-g}d^4x, \tag{1}$$

where $f(R)$ is an arbitrary functions of the Ricci scalar R. Since we are only interested in the vacuum case we do not add a matter Lagrangian to the action.

Varying the action with respect to the metric $g_{\mu\nu}$ yields the field equations, given by

$$F(R)R_{\mu\nu} - \frac{1}{2}f(R)g_{\mu\nu} - \nabla_\mu\nabla_\nu F(R) + g_{\mu\nu}\Box F(R) = 0, \tag{2}$$

where we have denoted $F(R) = df(R)/dR$. Note that the covariant derivative of these field equations vanishes for all $f(R)$ by means of the generalized Bianchi identities [17, 22].

In the following we will restrict our study of $f(R)$ gravity models to the static and spherically symmetric metric given by

$$ds^2 = -e^{\nu(r)}dt^2 + e^{\lambda(r)}dr^2 + r^2\left(d\theta^2 + \sin^2\theta d\phi^2\right). \tag{3}$$

For a metric of the form given by Eq. (3), the vacuum field equations of $f(R)$ gravity can be expressed as [23]

$$\frac{F''}{F} - \frac{1}{2}(\nu' + \lambda')\frac{F'}{F} - \frac{\nu' + \lambda'}{r} = 0, \tag{4}$$

$$\nu'' + \nu'^2 - \frac{1}{2}(\nu' + \lambda')\left(\nu' + \frac{2}{r}\right) - \frac{2}{r^2}(1 - e^\lambda) = -2\frac{F''}{F} + \left(\lambda' + \frac{2}{r}\right)\frac{F'}{F}, \tag{5}$$

$$\frac{f}{F}e^\lambda = -\nu'' - \frac{1}{2}(\nu' - \lambda')\nu' + \frac{2}{r}\lambda' + \left(\nu' + \frac{4}{r}\right)\frac{F'}{F}, \tag{6}$$

$$R = 2\frac{f}{F} - 3e^{-\lambda}\left[\frac{F''}{F} + \frac{1}{2}\left(\nu' - \lambda' + \frac{4}{r}\right)\frac{F'}{F}\right], \tag{7}$$

where the prime denotes differentiation with respect to r. Introducing a new variable ξ by means of the transformation $\xi = \ln r$, the field equations Eqs. (4) and (5) become

$$\frac{F_{,\,\xi\xi}}{F} - \left[1 + \frac{1}{2}(\nu_{,\,\xi} + \lambda_{,\,\xi})\right]\frac{F_{,\,\xi}}{F} - (\nu_{,\,\xi} + \lambda_{,\,\xi})F = 0\,, \tag{8}$$

$$\nu_{,\,\xi\xi} - \nu_{,\,\xi} + \nu_{,\,\xi}^2 - \frac{1}{2}(\nu_{,\,\xi} + \lambda_{,\,\xi})(\nu_{,\,\xi} + 2) + 2(1 - e^\lambda) = -2\frac{F_{,\,\xi\xi}}{F} + (\lambda_{,\,\xi} + 4)\frac{F_{,\,\xi}}{F}\,, \tag{9}$$

where the comma denotes differentiation with respect to the variable ξ. As a result of introducing the new independent variable the basic field equations Eqs. (4) and (5) are independent of the coordinate ξ. It is useful to introduce a formal representation of the function F as $F_{,\,\xi}/F = u$, $F_{,\,\xi\xi}/F = u_{,\,\xi} + u^2$, with u a new function of ξ. Then Eq. (4) can be written as

$$u_{,\,\xi} + u^2 - \left[1 + \frac{1}{2}(\nu_{,\,\xi} + \lambda_{,\,\xi})\right]u - (\nu_{,\,\xi} + \lambda_{,\,\xi}) = 0. \tag{10}$$

This equation is a Riccati type first order differential equation. By using the function u, Eq. (5) becomes

$$\nu_{,\,\xi\xi}-\nu_{,\,\xi}+\nu_{,\,\xi}^{2}-\frac{1}{2}(\nu_{,\,\xi}+\lambda_{,\,\xi})(\nu_{,\,\xi}+2)+2(1-e^{\lambda})=-2u_{,\,\xi}-2u^{2}+(\lambda_{,\,\xi}+4)u. \tag{11}$$

Substituting the term $u_{,\,\xi}+u^{2}$ in Eq. (11) with the use of Eq. (10), we obtain

$$2(1-e^{\lambda})+\nu_{,\,\xi\xi}-\nu_{,\,\xi}+\nu_{,\,\xi}^{2}+(\nu_{,\,\xi}+\lambda_{,\,\xi})(1-\frac{1}{2}\nu_{,\,\xi})-(2-\nu_{,\,\xi})u=0. \tag{12}$$

The general solution of Eqs. (10) and (12) gives the general solution of the field equations for the static vacuum case of the $f(R)$ gravity models. Once $\nu(\xi)$ and $\lambda(\xi)$ are specified, one can immediately obtain u and then (by integration) F, as well as all the other relevant physical quantities. If the function F and the metric tensor coefficients are known, f can be obtained as a function of R from Eqs. (6) and (7) in a parametric form, as $f=f\left(\xi\right)$, $R=R\left(\xi\right)$.

We now consider general solutions with $\nu_{,\,\xi}+\lambda_{,\,\xi}=0$, which we denote as Schwarzschild-type solutions. The constant of integration may be set to zero by re-scaling the time coordinate, so that without a significant loss of generality one may consider the solution $\nu+\lambda=0$. Thus, Eq. (10) reduces to $u_{,\,\xi}+u^{2}-u=0$, which provides the solution

$$u=\frac{e^{\xi}}{e^{\xi}+C}=\frac{r}{r+C}\,, \tag{13}$$

where C is a constant of integration. Next, from the definition of u, and by reverting back to the r coordinate, we obtain $F(r)=Ar+B$, with A and B constants of integration. Solving Eq. (12), one finds the Schwarzschild type general solution in $f(R)$ gravity, given by

$$\begin{aligned} e^{\nu} \;=\; e^{-\lambda} &= 1-\frac{AC_{2}}{2B^{2}}+\frac{C_{2}}{3Br}-\frac{A(B^{2}-AC_{2})}{B^{3}}r+\frac{1}{B^{2}}\left(A^{2}-\frac{C_{1}}{6B^{2}}\right)r^{2}+ \\ &\quad \frac{A^{2}(B^{2}-AC_{2})r^{2}}{B^{4}}\ln\left(A+\frac{B}{r}\right), \end{aligned} \tag{14}$$

where C_1 and C_2 are arbitrary constants of integration. An interesting difference to the vacuum solutions in general relativity is the presence of the linear term with respect to r, and of the term with the logarithmic dependence of r. In the general case the Schwarzschild type exact vacuum solution in $f(R)$ gravity depends on four arbitrary integration constants A, B, C_1 and C_2, respectively. In order to obtain the Schwarzschild-de Sitter solution of standard general relativity, one sets the following values for the constants: $A=0$, $C_2=-6BM$ and $C_1=2B^4\Lambda$, respectively, where M is the mass of the central object [23].

In the following we assume that $C_2 = -6BM$, a condition which is necessary to recover the standard Schwarzschild solution. Moreover, we neglect the possible effect of a cosmological constant by taking $C_1 = 0$. By denoting the ratio $A/B = 1/\eta$, we represent the vacuum metric in $f(R)$ gravity in the form

$$e^{\nu} = e^{-\lambda} = 1 + \frac{3M}{\eta} - \frac{2M}{r} - \left(1 + \frac{6M}{\eta}\right)\left(\frac{r}{\eta}\right) + \left(\frac{r}{\eta}\right)^2 \left\{1 + \left(1 + \frac{6M}{\eta}\right) \ln\left[A\left(1 + \frac{\eta}{r}\right)\right]\right\}. \tag{15}$$

By using the Schwarzschild-type solution of the field equations in the modified $f(R)$ gravity model given by Eqs. (15) we obtain for the functions $f(r)$, $R(r)$ and $dF/dR = d^2f/dR^2$ the following expressions

$$\begin{aligned} f(r) \; = \; & \frac{1}{\eta^2 (r+\eta) r^2} \left\{2A\eta \left[3(6M - r) r^2 + \eta r (9M + r)) - 3\eta^2 (M - r)\right]\right. \\ & \left. -6Ar^2 (6M + \eta)(r + \eta) \ln\left[A\left(1 + \eta r^{-1}\right)\right]\right\}, \end{aligned} \tag{16}$$

$$\begin{aligned} R(r) \; = \; & \frac{1}{\eta^3 (r+\eta)^2 r^2} \left\{\eta \left[6M(2r + \eta)\left(6r^2 + 6\eta r - \eta^2\right) + r\left(-12r^3 - 12\eta r^2 + 7\eta^2 r + 6\eta^3\right)\right]\right. \\ & \left. -12r^2 (6M + \eta)(r + \eta) \ln\left[A\left(1 + \eta r^{-1}\right)\right]\right\} \end{aligned} \tag{17}$$

and

$$\frac{dF}{dR} = \frac{d^2 f}{dR^2} = -\frac{Ar^3 (r+\eta)^3}{2r^3 + 6\eta r^2 + 6\eta^2 (r - 2M)} \tag{18}$$

respectively. Generally, the relation between f and R cannot be obtained in an explicit analytical form. However, some approximate representations are possible in the limiting cases of small and large r, respectively.

In the limit of small r, so that r is approximately equal to a few M, the logarithmic correction $\ln(A + B/r)$ becomes the dominant term, and we obtain $f(r) \approx -\chi_f^{-1} \ln B/r$, where $\chi_f = \eta^2/6A(6M + \eta)$, and $R(r) \approx -\chi_R (r + \eta)^{-1} \ln B/r$, where $\chi_R = 12(6M + \eta)/\eta^3$. By eliminating r using the relation $r = B\exp(-\chi_f f)$ we obtain

$$R = \frac{\chi_f \chi_R}{B\exp(-\chi_f f) + \eta} f. \tag{19}$$

If f is small we reobtain the Lagrangian of the standard general relativity, $f \sim R$. By performing a series expansion of the exponential factor we obtain

$$f(R) \approx \frac{B + \eta}{\chi_f} \frac{R}{BR + \chi_R} \approx \frac{B + \eta}{\chi_f \chi_R} R\left(1 - \frac{B}{\chi_R} R\right). \tag{20}$$

In the limit of large r, so that $r >> M$ and $r >> \eta$, by keeping only the terms in $1/r$, we obtain $f(r) \approx \chi_{f\infty} + 1/\eta r$, and $R(r) \approx \chi_{R\infty}/r - 12/\eta^2$, where $\chi_{f\infty} = -6\left[6\eta + (6M+\eta)\ln A\right]A$ and $\chi_{R\infty} = 12\left[6M\eta - \eta^2 - (6M+\eta)\ln A\right]/\eta^3$. Eliminating $1/r$ we obtain

$$f(R) = \frac{1}{\eta\chi_{R\infty}}R + \Lambda, \tag{21}$$

where $\Lambda = 12/\eta^3\chi_{R\infty} + \chi_{f\infty}$. Therefore at large distances the modified $f(R)$ gravity model generates a constant term, the cosmological constant, that is responsible for the accelerated expansion of the Universe.

Eqs. (16)-(18) can be used to discuss the conditions under which the generalized Schwarzschild type solution, as well as the corresponding $f(R)$ generalized gravity theory, represents a viable model. The conditions under which $f(R)$ theories can represent viable models of cosmic acceleration have been summarized in [24]. The requirement of the existence of a stable, high curvature regime imposes the constraint $d^2f/dR^2 > 0$, for $R >> d^2f/dR^2$. From Eq. (18) it follows that this condition can be satisfied for all r if $A < 0$ and $\eta > 0$. Moreover, the condition $(r/\eta)^3 + 3(r/\eta)^2 + 3(r/\eta) > 6M/\eta$ must also hold for all r, η and M. From the tight constraints of the Big Bang Nucleosynthesis and of the Cosmic Microwave Background we require that $F = df/dR$ must be a negative, monotonically increasing function of R that asymptotically approaches to zero from below. The condition $F = -Ar + B < 0$ can be used to constrain the range of the radial variable as $r > \eta$, where we have assumed that $B > 0$.

From the requirement that the effective Newton constant $G_{eff} = G/(1+F)$ is not allowed to change sign we obtain the condition $1 + F > 0$, at all finite R. This condition gives $r < \eta + 1/A$. Therefore in the present model the range of the radial variable r is restricted to $\eta < r < \eta + 1/A$. In order for the model to be viable on very large distances, corresponding to cosmic scales, A must have a very small numerical value. Finally, F must be a small quantity, a condition which is required for the model to pass the solar and galactic scale constraints. In terms of the scalar curvature R, the conditions of viability of the $f(R)$ gravity model with Schwarzschild like vacuum solution can be formulated, in the small r limit, as $-2B(B+\eta)/\chi_f\chi_R^2 < 0$ (condition which follows from $d^2f/dR^2 < 0$), $\chi_R/2B < R < \chi_R/2B + \chi_f\chi_R^2/2B(B+\eta)$, which follows from $df/dR < 0$ and $1 + df/dR > 0$, respectively.

Since A must be a very small (dimensionless) quantity, $A << 1$, the condition of the

smallness of F is automatically satisfied by also assuming a small numerical value for B. By assuming that the value of $|F|$ should not exceed today the numerical value of 10^{-6} at any point in the space-time [24], the requirement that the modified gravity model is viable on a scale of $r = 1000M$, for example, where M is the mass of the central black hole, and by representing B as $B = \beta M$, where β is a constant, gives the condition $\beta - 1000A = 10^{-6}/M$. For a black hole with a mass of around three solar masses we obtain $\beta - 1000A \approx 6.74 \times 10^{-12}$. For $\beta = 1$ it follows that A is very close to $A \approx 10^{-3}$.

III. THIN ACCRETION DISKS ONTO BLACK HOLES

For the thin accretion disk it is assumed that its horizontal size is negligible as compared to its vertical extension, i.e, the disk height H, defined by the maximum half thickness of the disk, is always much smaller than the characteristic radius r of the disk, $H << r$. The thin disk is in hydrodynamical equilibrium, where there is only negligible pressure gradient and a vertical entropy gradient in the accreting matter. The efficient cooling via the radiation over the disk surface prevents the disk from cumulating the heat generated by stresses and dynamical friction. In turn this equilibrium causes the disk to stabilize its thin vertical size. The thin disk has an inner edge at the marginally stable orbit of the black hole potential, and the accreting plasma has a Keplerian motion in higher orbits.

In steady state accretion disk models, the mass accretion rate $\dot{M}_0$ is assumed to be a constant that does not change with time, and the physical quantities describing the orbiting plasma are averaged over a characteristic time scale, e.g. Δt, over the azimuthal angle $\Delta\phi = 2\pi$ for a total period of the orbits, and over the height H [27, 28, 29].

The particles moving in Keplerian orbits around the black hole with a rotational velocity $\Omega = d\phi/dt$ have a specific energy $\widetilde{E}$ and a specific angular momentum $\widetilde{L}$, which, in the steady state thin disk model, depend only on the radii of the orbits. These particles, orbiting with the four-velocity u^μ, form a disk of an averaged surface density Σ, the vertically integrated average of the rest mass density ρ_0 of the plasma. The accreting matter in the disk is modelled by an anisotropic fluid source, where the density ρ_0 , the energy flow vector q^μ and the stress tensor $t^{\mu\nu}$ are measured in the averaged rest-frame (the specific heat was neglected). Then the disc structure can be characterized by the surface density of the disk

[27, 29],

$$\Sigma(r) = \int_{-H}^{H} \langle \rho_0 \rangle dz, \tag{22}$$

with averaged rest mass density $\langle \rho_0 \rangle$ over Δt and 2π and the torque

$$W_\phi{}^r = \int_{-H}^{H} \langle t_\phi{}^r \rangle dz, \tag{23}$$

with the averaged component $\langle t_\phi^r \rangle$ over Δt and 2π. The time and orbital average of the energy flux vector gives the radiation flux $\mathcal{F}(r)$ over the disk surface as $\mathcal{F}(r) = \langle q^z \rangle$.

The stress-energy tensor is decomposed according to

$$T^{\mu\nu} = \rho_0 u^\mu u^\nu + 2u^{(\mu} q^{\nu)} + t^{\mu\nu}, \tag{24}$$

where $u_\mu q^\mu = 0$, $u_\mu t^{\mu\nu} = 0$. The four-vectors of the energy and angular momentum flux are defined by $-E^\mu \equiv T^\mu_\nu (\partial/\partial t)^\nu$ and $J^\mu \equiv T^\mu_\nu (\partial/\partial\phi)^\nu$, respectively. The structure equations of the thin disk can be derived by integrating the conservation laws of the rest mass, of the energy, and of the angular momentum of the plasma, respectively [27, 29]. From the equation of the rest mass conservation, $\nabla_\mu(\rho_0 u^\mu) = 0$, it follows that the time averaged rate of the accretion of the rest mass is independent of the disk radius,

$$\dot{M}_0 \equiv -2\pi r \Sigma u^r = \text{constant}. \tag{25}$$

The conservation law $\nabla_\mu E^\mu = 0$ of the energy has the integral form

$$[\dot{M}_0 \widetilde{E} - 2\pi r \Omega W_\phi{}^r]_{,r} = 4\pi r \mathcal{F} \widetilde{E} \ , \tag{26}$$

which states that the energy transported by the rest mass flow, $\dot{M}_0 \widetilde{E}$, and the energy transported by the dynamical stresses in the disk, $2\pi r \Omega W_\phi{}^r$, is in balance with the energy radiated away from the surface of the disk, $4\pi r \mathcal{F} \widetilde{E}$. The law of the angular momentum conservation, $\nabla_\mu J^\mu = 0$, also states the balance of these three forms of the angular momentum transport,

$$[\dot{M}_0 \widetilde{L} - 2\pi r W_\phi{}^r]_{,r} = 4\pi r \mathcal{F} \widetilde{L} \ . \tag{27}$$

By eliminating $W_\phi{}^r$ from Eqs. (26) and (27), and applying the universal energy-angular momentum relation $dE = \Omega dJ$ for circular geodesic orbits in the form $\widetilde{E}_{,r} = \Omega \widetilde{L}_{,r}$, the flux $\mathcal{F}$ of the radiant energy over the disk can be expressed in terms of the specific energy, angular momentum and of the angular velocity of the black hole [27, 29],

$$\mathcal{F}(r) = -\frac{\dot{M}_0}{4\pi r} \frac{\Omega_{,r}}{(\widetilde{E} - \Omega \widetilde{L})^2} \int_{r_{ms}}^{r} (\widetilde{E} - \Omega \widetilde{L}) \widetilde{L}_{,r} dr \ . \tag{28}$$

In the derivation of the above formula the "no torque" inner boundary condition were prescribed, where the torque vanishes at the inner edge of the disk. Thus, we assume that the accreting matter at the marginally stable orbit r_{ms} falls freely into the black hole, and cannot exert considerable torque on the disk. The latter assumption is valid only if strong magnetic fields do not exist in the plunging region, where matter falls into the black hole.

Another important characteristics of the mass accretion process is the efficiency with which the central object converts rest mass into outgoing radiation. This quantity is defined as the ratio of the rate of the radiation of energy of photons escaping from the disk surface to infinity, and the rate at which mass-energy is transported to the black hole, both measured at infinity [27, 29]. If all the emitted photons can escape to infinity, the efficiency is given in terms of the specific energy measured at the marginally stable orbit r_{ms},

$$\epsilon = 1 - \widetilde{E}_{ms}. \tag{29}$$

For Schwarzschild black holes the efficiency ϵ is about 6%, whether the photon capture by the black hole is considered, or not. Ignoring the capture of radiation by the hole, ϵ is found to be 42% for rapidly rotating black holes, whereas the efficiency is 40% with photon capture in the Kerr potential [30].

In order to compute the flux integral given by Eq. (28), we determine the radial dependence of the angular velocity Ω, of the specific energy $\widetilde{E}$ and of the specific angular momentum $\widetilde{L}$ of particles moving in circular orbits around black holes in the static and spherically symmetric geometry given by Eq. (3). The geodesic equations for particles orbiting in the equatorial plane of the black hole can be written as

$$e^{2\nu}\dot{t}^2 = \widetilde{E}^2, e^{(\nu+\lambda)}\dot{r}^2 + V_{eff}(r) = \widetilde{E}^2, r^4\dot{\phi}^2 = \widetilde{L}^2, \tag{30}$$

where the dot denotes the differentiation with respect to the affine parameter, and the effective potential is given by

$$V_{eff}(r) \equiv e^{\nu}\left(1 + \frac{\widetilde{L}^2}{r^2}\right) . \tag{31}$$

From the conditions $V_{eff}(r) = 0$ and $V_{eff,\,r}(r) = 0$ we obtain

$$\Omega = \sqrt{\frac{\nu_{,r}e^{\nu}}{2r}}\,, \tag{32}$$

$$\widetilde{E} = \frac{e^{\nu}}{\sqrt{e^{\nu} - r^2\Omega^2}}\,, \tag{33}$$

$$\widetilde{L} = \frac{r^2\Omega}{\sqrt{e^{\nu} - r^2\Omega^2}}\,. \tag{34}$$

The condition $V_{eff,\,rr}(r) = 0$ gives the marginally stable orbit r_{ms} (or the innermost stable circular orbit), which can be determined for any explicit expression of the function $\nu(r)$.

It is possible to define a temperature $T(r)$ of the disk, by using the definition of the flux, as $\mathcal{F}(r) = \sigma T^4(r)$, where σ is the Stefan-Boltzmann constant. Considering that the disk emits as a black body, one can use the dependence of T on $\mathcal{F}$ to calculate the luminosity $L(\omega)$ of the disk through the expression for the black body spectral distribution [32],

$$L(\omega) = 4\pi d^2 I(\omega) = \frac{4}{\pi}\cos i\omega^3 \int_{r_i}^{r_f} \frac{r dr}{\exp(\omega/T) - 1}, \tag{35}$$

where d is the distance to the source, $I(\omega)$ is the Planck distribution function, i is the disk inclination, and r_i and r_f indicate the position of the inner and outer edge of the disk, respectively.

IV. THIN DISK ACCRETION PROPERTIES FOR $f(R)$ MODIFIED GRAVITY BLACK HOLES

The effective potential which determines the geodesic motion of the test particles in the equatorial plane of the metric given by Eq. (15) can be written as

$$V_{eff}(r) = \left(1 + \frac{\widetilde{L}^2}{r^2}\right)\left\{1 + \frac{3M}{\eta} - \frac{2M}{r} - \left(1 + \frac{6M}{\eta}\right)\left(\frac{r}{\eta}\right) + \left(\frac{r}{\eta}\right)^2 + \left(\frac{r}{\eta}\right)^2\left(1 + \frac{6M}{\eta}\right)\ln\left[A\left(1 + \frac{\eta}{r}\right)\right]\right\}. \tag{36}$$

We plot V_{eff} for different parameters A (or η) in Fig. 1. Here the parameter A runs over the range of -3×10^{-3} and 3×10^{-3} in each plot whereas B is set to M, $2M$, $3M$ and $4M$, so that $\eta = M/A, 2M/A, 3M/A$ and $4M/A$, respectively. The effective potential of the Schwarzschild solution is also plotted for comparison.

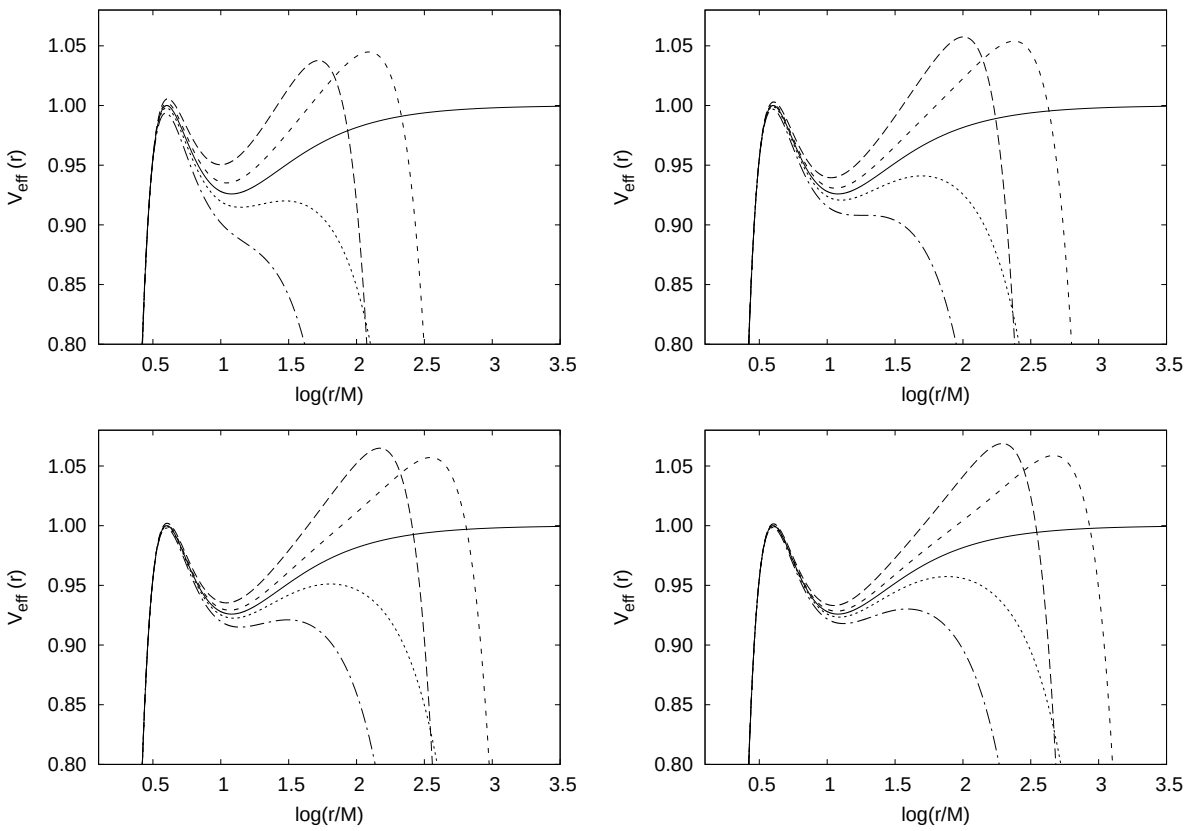

FIG. 1: The effective potential $V_{eff}(r)$ for a black hole of total mass $M = 2.5 \times 10^6 M_{\odot}$ and for the specific angular momentum $\widetilde{L} = 4M$. The metric parameter A is varied in the range of -3×10^{-3} and 3×10^{-3} for fixed B in each plot. The parameter B is set to M (the left hand upper plot), $2M$ (the right hand upper plot), $3M$ (the left hand lower plot) and $4M$ (the right hand lower plot), respectively. The solid line is the effective potential for a Schwarzschild black hole with the total mass M. The various values of A are -3×10^{-3} (long dashed line), -10^{-3} (short dashed line), 10^{-3} (dotted line) and 3×10^{-3} (dot-dashed line).

The unique singular behavior of $V_{eff}(r)$ at the spatial infinity, as opposed to the asymptotical fall-off of the Schwarzschild potential, is the most striking feature in the upper pairs of the plots, where all the curves representing the $f(R)$ potential for different parameters tend to $-\infty$ as $r \to \infty$. This is only a pure manifestation of the global properties of the spacetime for vacuum $f(R)$ gravity models. It is also true for the cases in the lower two panels, where the curves plotted above the Schwarzschild limit go to $-\infty$ at the spatial infinity, after reaching a local maximum at the marginally bound orbit. This indicates the obvious fact that though the metric parameters considerably determine the local properties

of the gravitational field, the globally hyperbolic geometry must be insensitive to them.

This behavior of the potential in the $f(R)$ modified gravity models directly follows from the presence of the logarithmic correction term in V_{eff}, and does not depend on the sign of the parameters A and B. In the case of a small negative value of A, for some critical value of r the argument of the logarithm tends to zero, and the logarithmic term dominates all the other terms in the potential, which behaves like $V_{eff}(r) \approx (r/\eta)^2 (1 + 6M/\eta) \ln(-A + B/r)$ (the minus sign is due to the smallness of the argument of the logarithmic function $-A + B/r$). Interestingly, the same behavior appears if A is a small positive number. In this case for $B/r \to 0$, the potential behaves like $V_{eff}(r) \approx (r/\eta)^2 (1 + 6M/\eta) \ln A$. Due to the smallness of A, the potential tends again, in the large r limit, to $-\infty$.

By fixing the parameter B and increasing A from small negative values to zero, we deepen the potential well between the marginally stable orbit (indicated by the peak in the left hand side), and the marginally bound orbit r_{mb} (at the local maximum in the right hand side of the potential well). At $A = 0$ we reach the Schwarzschild geometry and for $A > 0$ we obtain deeper potential well, and reduce the local maximum further till it becomes an inflexion point. As a result, for any non zero value of A, we can only decrease the radial distance between r_{ms} and r_{mb}, as compared to the case of the Schwarzschild potential. Therefore, the domain between the two radii for the Keplerian motion of the matter will be decreased as well.

The physical implications of this effect, specific to modified $f(R)$ gravity models, can be studied in detail in Figs. 2, where we have plotted the energy flux emitted by the accretion disk for the same values of metric parameters A and B.

The cut-offs of the radial flux profiles in the right hand side at r_{mb} always appear, no matter if the values of A are positive or negative. However, the sign of the values of A is already important for the direction of the change of the intensity, as compared to the Schwarzschild geometry. Since the potential well is deeper for $A > 0$, the specific energies of the orbiting particles are lower, which decreases the radiated flux over the disk surface. For negative values of A we have the opposite effect: in the higher potential well the particles have higher specific energies, and more energy is radiated away than in the previous case.

These effects in the disk radiation can also be observed in the emission spectrum of the accretion disk, plotted in Figs. 3.

In the lower regime, up to the cut-off frequency of the spectrum at about 10^{16} Hz, the

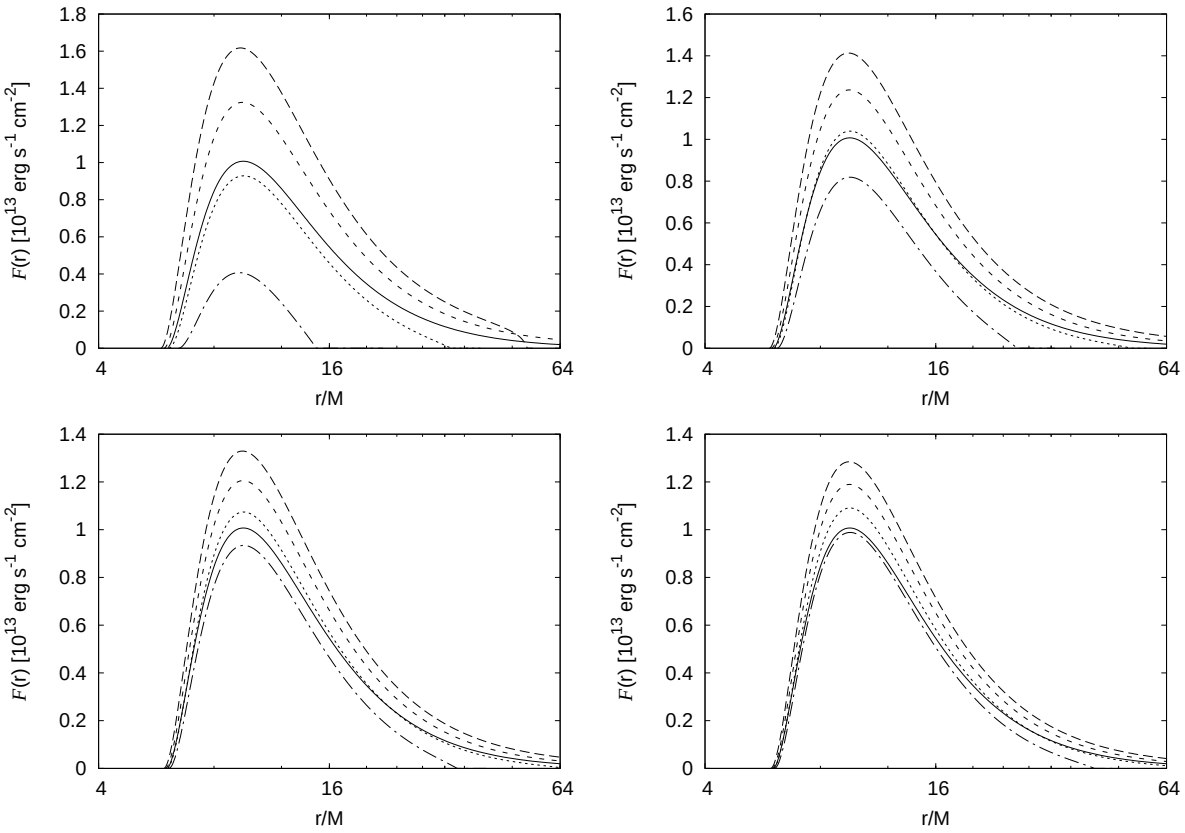

FIG. 2: The time averaged flux $\mathcal{F}(r)$ radiated by the disk for a black hole of total mass $M = 2.5 \times 10^6 M_{\odot}$. The parameter B is set to M (the upper left hand plot), $2M$ (the upper right hand plot), $3M$ (the lower left hand plot) and $4M$ (the lower right hand plot), respectively. The solid line is the energy flux for a Schwarzschild black hole with total mass M. The various values of A are -3×10^{-3} (long dashed line), -10^{-3} (short dashed line), 10^{-3} (dotted line) and 3×10^{-3} (dot-dashed line).

disk emission is much lower for $f(R)$ black holes than for the Schwarzschild black hole. As A tends to zero, the intensity is of course raising up, and approaches the solid line representing the case of the Schwarzschild black hole. For frequencies higher than the cut-off value, the differences are not so striking, but still observable. For negative values of A, the cut-off in the spectrum shifts to higher frequencies, whereas positive values of A produce lower cut-off frequency. The effect of varying the parameter B is also important, as all these differences are more striking for lower values of B, as can be seen by comparing the upper left hand plot, for $B = M$, with the lower right hand one, corresponding to $B = 4M$. For all the cases we have considered here, the smaller values of the emission at lower frequencies have

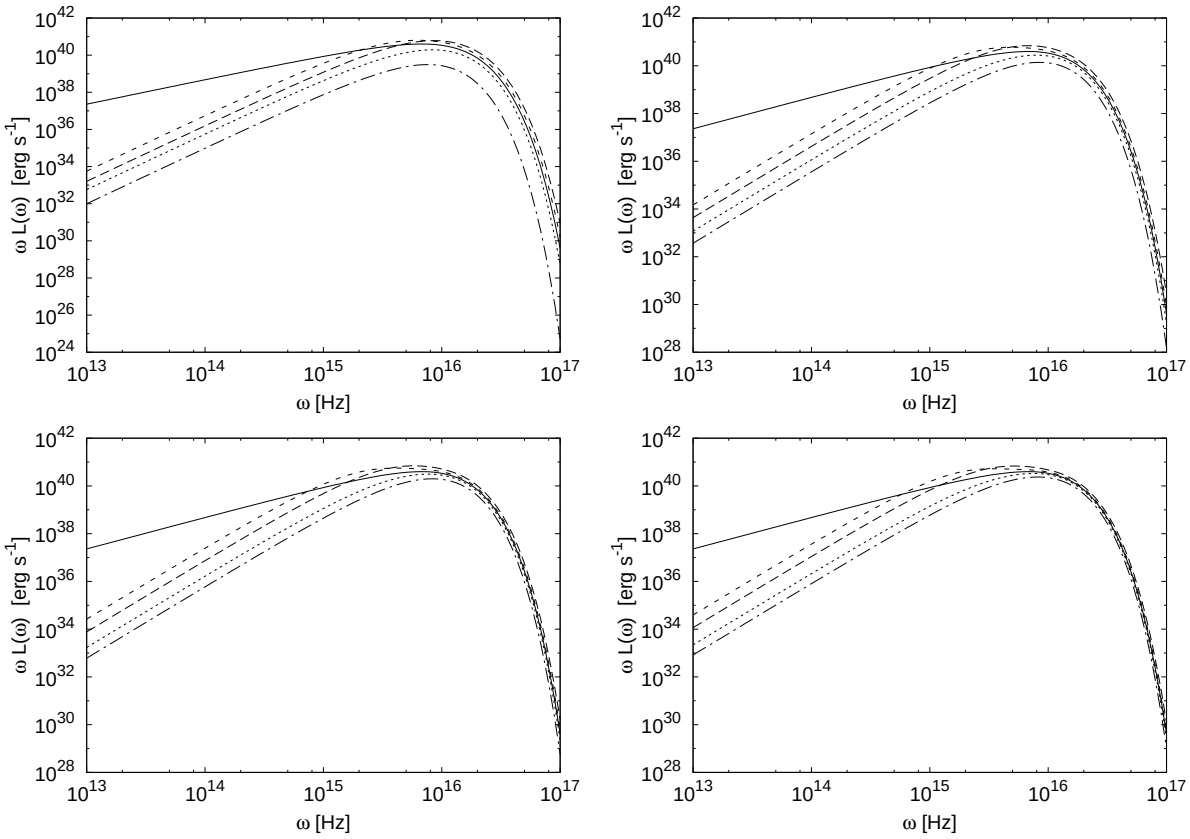

FIG. 3: Emission spectra $\omega L(\omega)$ of disks for a black hole of total mass $M = 2.5 \times 10^6 M_{\odot}$. The accretion disk is aligned into a face-on position, with $\cos i = 1$. The parameter B is set to M (the left hand upper plot), $2M$ (the upper right upper plot), $3M$ (the upper left hand plot) and $4M$ (the lower right hand plot), respectively. The solid line is the emission spectrum for a Schwarzschild black hole, with the same total mass M. The various values of A are -3×10^{-3} (long dashed line), -10^{-3} (short dashed line), 10^{-3} (dotted line) and 3×10^{-3} (dot-dashed line).

the consequence of hardening the disk emission spectrum. The emission spectrum is slightly modified due to the effects of varying A, from small negative values to positive ones, which softens the emission as we reach positive values of A.

We also present the conversion efficiency ϵ of the accreting mass into radiation, measured at infinity, which is given by Eq. (29), for the case where the photon capture by the hole is ignored. The value of ϵ measures the efficiency of energy generating mechanism by mass accretion. The amount of energy released by matter leaving the marginally stable orbit, and falling down the black hole, is the binding energy $\widetilde{E}_{ms}$ of the black hole potential. For different metric parameters A and B, the values of $\widetilde{E}_{ms}$ are given, together with the radii of

A	$B\ [M]$	$r_{ms}\ [M]$	ϵ
0	-	6.0000	0.0572
-3×10^{-3}	1	5.8154	0.0454
-10^{-3}	1	5.9218	0.0531
10^{-3}	1	6.1044	0.0616
3×10^{-3}	1	6.4706	0.0712
-3×10^{-3}	2	5.8861	0.0510
-10^{-3}	2	5.978	0.0551
10^{-3}	2	6.0489	0.0593
3×10^{-3}	2	6.1700	0.0638
-3×10^{-3}	3	5.9218	0.0530
-10^{-3}	3	5.9759	0.0558
10^{-3}	3	6.0398	0.0586
3×10^{-3}	3	6.1044	0.0615
-3×10^{-3}	4	5.9398	0.0540
-10^{-3}	4	5.9850	0.0561
10^{-3}	4	6.0306	0.0583
3×10^{-3}	4	6.0766	0.0604

TABLE I: The marginally stable orbit and the efficiency for different $f(R)$ black hole geometries. The case $A = 0$ corresponds to the standard Schwarzschild general relativistic black hole.

the marginally stable orbits, in Table I, where the figures corresponding to the Schwarzschild black hole appear in the first line. For $A < 0$ both the r_{ms} and ϵ are smaller than those for the Schwarzschild potential, whereas we obtain higher values than 6 and 0.0572 for $A > 0$. Nevertheless, the efficiency is decreasing with the increasing values of B. For $B = 4M$ the values of ϵ are about 10 percent smaller than those for $B = M$.

V. DISCUSSIONS AND FINAL REMARKS

In the present paper we have considered the basic physical properties of matter forming a thin accretion disc in the Schwarzschild type vacuum space-time metric of the $f(R)$ modified gravity models. The physical parameters of the disc - effective potential, flux and emission spectrum profiles - have been explicitly obtained for several values of the parameters characterizing the vacuum solution of the generalized field equations. All the astrophysical quantities, related to the observable properties of the accretion disc, can be obtained from the black hole metric. Due to the differences in the space-time structure, the modified $f(R)$ gravity black holes present some very important differences with respect to the disc properties as compared to the standard general relativistic Schwarzschild case.

The determination of the accretion rate for an astrophysical object can give a strong evidence for the existence of a surface of the object. A model in which Sgr A*, the $3.7 \times 10^6 M_{\odot}$ super massive black hole candidate at the Galactic center, may be a compact object with a thermally emitting surface was considered in [34]. For very compact surfaces within the photon orbit, the thermal assumption is likely to be a good approximation because of the large number of rays that are strongly gravitationally lensed back onto the surface. Given the very low quiescent luminosity of Sgr A* in the near-infrared, the existence of a hard surface, even in the limit in which the radius approaches the horizon, places a severe constraint on the steady mass accretion rate onto the source, $\dot{M} \leq 10^{-12} M_{\odot}$ yr^{-1}. This limit is well below the minimum accretion rate needed to power the observed submillimeter luminosity of Sgr A*, $\dot{M} \geq 10^{-10} M_{\odot}$ yr^{-1}.

Thus, from the determination of the accretion rate it follows that Sgr A* does not have a surface, that is, it must have an event horizon. Therefore the study of the accretion processes by compact objects is a powerful indicator of their physical nature. Since, as one can see from Table I, the conversion efficiency in the case of the $f(R)$ vacuum solutions is different as compared to the general relativistic case, the determination of this parameter could discriminate, at least in principle, between the different gravity theories, and constrain the parameters of the model.

Acknowledgments

The work of T. H. is supported by an RGC grant of the government of the Hong Kong SAR. Z. K. is indebted to the colleagues in the Department of Physics of the University of Hong Kong for their support and warm hospitality during the preparation of this work.

---

[1] A. G. Riess et al., Astron. J. **116**, 1009 (1998); S. Perlmutter et al., Astrophys. J. **517**, 565 (1999); P. de Bernardis et al., Nature **404**, 955 (2000); S. Hanany et al., Astrophys. J. **545**, L5 (2000).

[2] P. J. E. Peebles and B. Ratra, Rev. Mod. Phys. **75**, 559 (2003); T. Padmanabhan, Phys. Repts. **380**, 235 (2003).

[3] H. A. Buchdahl, Mon. Not. Roy. Astron. Soc. **150**, 1 (1970); R. Kerner, Gen. Rel. Grav. **14**, 453 (1982); J. P. Duruisseau, R. Kerner and P. Eysseric, Gen. Rel. Grav. **15**, 797 (1983); J. D. Barrow and A. C. Ottewill, J. Phys. A: Math. Gen. **16**, 2757 (1983).

[4] S. M. Carroll, V. Duvvuri, M. Trodden and M. S. Turner, Phys. Rev. D **70**, 043528 (2004).

[5] S. Capozziello, S. Nojiri, S. D. Odintsov and A. Troisi, Phys. Lett. **B 639**, 135 (2006); L. Amendola, D. Polarski and S. Tsujikawa, Phys. Rev. Lett. **98**, 131302 (2007); S. Capozziello, S. Nojiri, S. D. Odintsov and A. Troisi, Phys. Lett. **B639**, 135 (2006); S. Nojiri and S. D. Odintsov, Phys. Rev. **D74**, 086005 (2006); M. Amarzguioui, O. Elgaroy, D. F. Mota and T. Multamaki, Astron. Astrophys. **454**, 707 (2006); L. Amendola, R. Gannouji, D. Polarski and S. Tsujikawa, Phys. Rev. **D75**, 083504 (2007); T. Koivisto, Phys. Rev. D **76**, 043527 (2007); A. A. Starobinsky, JETP Lett. **86**, 157 (2007); B. Li, J. D. Barrow and D. F. Mota, Phys. Rev. D **76**, 044027 (2007); S. E. Perez Bergliaffa, Phys. Lett. **B642**, 311 (2006); J. Santos, J. S. Alcaniz, M. J. Reboucas and F. C. Carvalho, Phys. Rev. D **76**, 083513 (2007); G. Cognola, E. Elizalde, S. Nojiri, S. D. Odintsov and S. Zerbini, JCAP **0502**, 010 (2005); V. Faraoni, Phys. Rev. **D72**, 061501 (2005); V. Faraoni, Phys. Rev. **D72**, 124005 (2005); S. Nojiri and S. D. Odintsov, Int. J. Geom. Meth. Mod. Phys. **4**, 115 (2007); L. M. Sokolowski, Class. Quantum Grav. **24**, 3391 (2007); V. Faraoni, Phys. Rev. **D75**, 067302 (2007); G. Cognola, E. Elizalde, S. Nojiri, S. D. Odintsov, L. Sebastiani and S. Zerbini, [gr-qc/0712.4017] (2007); C. G. Böhmer, L. Hollenstein and F. S. N. Lobo, Phys. Rev. D **76**, 084005 (2007); S. Carloni, P. K. S. Dunsby and A. Troisi,

arXiv:0707.0106 [gr-qc] (2007); S. Capozziello, R. Cianci, C. Stornaiolo and S. Vignolo, Class. Quant. Grav. **24**, 6417 (2007); S. Nojiri, S. D. Odintsov and P. V. Tretyakov, Phys. Lett. B **651**, 224 (2007); S. Nojiri and S. D. Odintsov, Phys. Lett. B **652**, 343 (2007); S. Tsujikawa, Phys. Rev. D **77**, 023507 (2008) ; K. N. Ananda, S. Carloni and P. K. S. Dunsby, Phys. Rev. **D77**, 024033 (2008).

[6] T. Chiba, Phys. Lett. **B575**, 1 (2003); A. L. Erickcek, T. L. Smith and M. Kamionkowski, Phys. Rev. **D74**, 121501 (2006); T. Chiba, T. L. Smith and A. L. Erickcek, Phys. Rev. **D75**, 124014 (2007). S. Nojiri and S. D. Odintsov, arXiv:0708.0924 [hep-th] (2007); S. Capozziello, A. Stabile and A. Troisi, arXiv:0708.0723 [gr-qc] (2007); S. Capozziello, A. Stabile and A. Troisi, arXiv:0709.0891 [gr-qc] (2007).

[7] G. J. Olmo, Phys. Rev. **D75**, 023511 (2007).

[8] T. P. Sotiriou, Gen. Rel. Grav. **38**, 1407 (2006); W. Hu and I. Sawicki, Phys. Rev. **D76**, 064004 (2007).

[9] S. Nojiri and S. D. Odintsov, Phys. Rev. **D68**, 123512 (2003); V. Faraoni, Phys. Rev. **D74**, 023529 (2006); T. Faulkner, M. Tegmark, E. F. Bunn and Y. Mao, Phys. Rev. **D76**, 063505 (2007); P. J. Zhang, Phys. Rev. D **76**, 024007 (2007); S. Capozziello and S. Tsujikawa, arXiv:0712.2268 [gr-qc].

[10] O. Mena, J. Santiago and J. Weller, Phys. Rev. Lett. **96**, 041103 (2006); I. Sawicki and W. Hu, Phys. Rev. **D75**, 127502 (2007).

[11] A. de la Cruz-Dombriz and A. Dobado, Phys. Rev. **D74**, 087501 (2006); S. Nojiri and S. D. Odintsov, Phys. Rev. **D74**, 086005 (2006); L. Amendola and S. Tsujikawa, 0705.0396 [astro-ph] (2007).

[12] S. Capozziello, V. F. Cardone and A. Troisi, JCAP **0608**, 001 (2006); S. Capozziello, V. F. Cardone and A. Troisi, Mon. Not. R. Astron. Soc. **375**, 1423 (2007).

[13] A. Borowiec, W. Godlowski and M. Szydlowski, Int. J. Geom. Meth. Mod. Phys. **4** (2007) 183

[14] C. F. Martins and P. Salucci, arXiv:astro-ph/0703243 (2007).

[15] C. G. Boehmer, T. Harko and F. S. N. Lobo, arXiv:0709.0046 [gr-qc] (2007).

[16] C. G. Boehmer, T. Harko and F. S. N. Lobo, JCAP **03**, 024 (2008).

[17] O. Bertolami, C. G. Boehmer, T. Harko and F. S. N. Lobo, Phys. Rev. **D75**, 104016 (2007).

[18] O. Bertolami and J. Paramos, arXiv:0709.3988 [astro-ph]; V. Faraoni, Phys. Rev. D **76**, 127501 (2007); O. Bertolami and J. Paramos, arXiv:0805.1241 (2008); T. P. Sotiriou, arXiv:0805.1160

(2008); T. P. Sotiriou and V. Faraoni, arXiv:0805.1249 (2008).

[19] T. P. Sotiriou and V. Faraoni, arXiv:0805.1726 (2008).

[20] T. Multamaki and I. Vilja, Phys. Rev. D **76**, 064021 (2007).

[21] S. Capozziello, A. Stabile and A. Troisi, Class. Quant. Grav. **24**, 2153 (2007); S. Capozziello, A. Stabile and A. Troisi, Phys. Rev. D **76**, 104019 (2007); K. Kainulainen, J. Piilonen, V. Reijonen and D. Sunhede, Phys. Rev. D **76**, 024020 (2007); K. Henttunen, T. Multamaki and I. Vilja, arXiv:0705.2683 [astro-ph] (2007); T. Multamaki and I. Vilja, arXiv:0709.3422 [astro-ph] (2007).

[22] T. Koivisto, Class. Quant. Grav. **23**, 4289 (2006).

[23] T. Multamaki and I. Vilja, Phys. Rev. D **74**, 064022 (2006).

[24] L. Pogosian and A. Silvestri, arXiv:0709.0296 (2007).

[25] C. M. Urry and P. Padovani, Publ. Astron. Soc. of the Pacific **107**, 803 (1995).

[26] M. Miyoshi, J. Moran, J. Herrnstein, L. Greenhill, N. Nakai, P. Diamond and M. Inoue, Nature **373**, 127 (1995).

[27] I. D. Novikov and K. S. Thorne, in Black Holes, ed. C. DeWitt and B. DeWitt, New York: Gordon and Breach (1973).

[28] N. I. Shakura and R. A. Sunyaev, Astron. Astrophys. **24**, 33 (1973).

[29] D. N. Page and K. S. Thorne, Astrophys. J. **191**, 499 (1974).

[30] K. S. Thorne, Astrophys. J. **191**, 507 (1974).

[31] S. Bhattacharyya, A. V. Thampan and I. Bombaci, Astron. Astrophys. **372**, 925 (2001).

[32] D. Torres, Nucl. Phys. B **626**, 377 (2002).

[33] Y. F. Yuan, R. Narayan and M. J. Rees Astrophys. J. **606**, 1112 (2004).

[34] A. E. Broderick and R. Narayan, Astrophys. J. **638**, L21 (2006).